Supercond. Sci. Technol. **22** (2009) 034010 (8pp) doi:10.1088/0953-2048/22/3/034010

Electric field effect and superconducting–insulating transition in '123' cuprate superconductors

M Salluzzo[1], G M De Luca[1], R Di Capua[1,2], A Gambardella[1], Z Ristic[1] and R Vaglio[1]

[1] CNR-INFM COHERENTIA and Department of Physics, University 'Federico II' of Naples, Complesso MonteSantangelo via Cinthia, I-80126 Napoli, Italy
[2] Dipartimento Scienze per la Salute, Università del Molise, Via De Sanctis, I-86100 Campobasso, Italy

Received 15 August 2008, in final form 2 October 2008
Published 6 February 2009
Online at stacks.iop.org/SUST/22/034010

Abstract

The physics of high critical temperature superconductors (HTS) remains a fascinating but undisclosed issue in condensed matter. One of the most interesting topics is the transition from the insulating phase of the parent compound, having long range antiferromagnetic order, to the superconducting phase. A method to investigate in detail the superconducting to insulating (SIT) transition in HTS is to control the doping of the CuO_2 planes in a fine way. Here, by using the electric field effect on thin $Nd_1Ba_2Cu_3O_7$ films, we present a study of the HTS phase diagram close to the SIT with unprecedented detail. By virtue of these data, we will show that doping of holes in samples located at the boundary separating the superconducting and insulating regions produces changes in the transport characteristic consistent with an electronic phase separation scenario. Some consequences of these data are the failure of standard 2D quantum scaling theory and the possible coexistence of superconducting and weakly insulating phases in this region of the phase diagram. A continuous transition between the two competing phases as a function of doping place evident constraints on the mechanism of superconductivity.

(Some figures in this article are in colour only in the electronic version)

1. Introduction

Understanding the superconducting to insulating transition (SIT) in high critical temperature superconductors (HTS) remains one of the most fascinating issues in condensed matter physics. The generality of the temperature versus doping HTS phase diagram suggests that understanding the region near the critical doping of 0.05 holes per CuO_2 plane could effectively throw some light on this subject. Parent undoped compounds are characterized by long range antiferromagnetic order, well explained by a 2D square lattice quantum Heisenberg antiferromagnet, due to the ordering of the $S = 1/2$ Cu $3d^9$ spin [1]. A small amount of holes, induced by chemical doping, creates a Zhang–Rice singlet and destroys the long range magnetic order [2]. Superconductivity sets in when a sufficient number of holes are introduced in the CuO_2 planes. Antiferromagnetism and superconductivity seem then antagonistic and a clear separation between the two phases is expected. However, it has been clearly established that HTS show signatures of inhomogeneous superconductivity even in optimally doped and slightly overdoped samples, as shown by the real-space distribution of the superconducting gap as observed by scanning tunneling spectroscopy (STS) [3]. One debated issue concerns the possibility that the high critical temperature superconductivity is intrinsically inhomogeneous. For example, it is believed that in underdoped samples the pseudogap phase coexists with the superconducting phase. In particular Fermi arcs with lengths depending on the actual doping replace a complete Fermi surface in the system, indicating that in some region of the reciprocal space quasiparticle spectral weight is missing [4]. The phenomena could also be attributed to the intrinsic doping mechanism of the CuO_2 planes, which occurs by cation substitution or by changes in the oxygen stoichiometry. Doping of the CuO_2 planes occurs by the transfer of holes (or extraction of electrons) into the (out of the) planes, a method to reduce the electrostatic Madelung potential. A similar mechanism has been proposed to explain the creation of an electron gas at the

artificial interface between $SrTiO_3$ and $LaAlO_3$ to avoid the 'polarization catastrophe' [5].

The chemical doping is intrinsically inhomogeneous and modifies the disorder in the system by creating, outside the CuO_2 planes in the charge reservoir, a random Coulomb field that is strongly dependent on the distribution of the doping ions. A modification of such a distribution is believed to affect the superconductivity by naturally creating a charge inhomogeneity inside the CuO_2 planes. Trying to control the doping distribution is the general approach used to study the HTS phase diagram. However, this method requires the synthesis of samples which naturally differ in terms of chemical order and structure. An alternative method consists in realizing field effect devices using a thin HTS epitaxial film as a drain to source channel. The gate voltage of such devices would serve as a reversible external parameter that controls the doping of the CuO_2 planes. One of the advantages of the field effect doping is that chemical disorder is frozen and the electric field is spatially uniform. Disorder is expected to be not modified in an electric field effect experiment.

In a naive picture, taken from the physics of metal oxide semiconducting field effect transistors (MOSFET), the charges accumulated at the interface between the gate dielectric and the thin HTS film would create carriers in the Zhang–Rice band, i.e. in the CuO_2 planes. Field effect doping in superconductors has been applied to amorphous bismuth (believed to be BCS superconductors) [6] and to HTS thin films [7–9]. Since the carrier density of HTS is much reduced compared to ordinary metals, technologically accessible external gate electric fields could effectively produce substantial changes in the doping, if the polarization charges are directly transformed into carriers. The whole HTS phase diagram could be accessible and therefore this could lead to easily controllable changes of T_c and to phase transitions. Although modulation of the T_c [8, 9] and of the critical current density [10] has been observed, the extent of the electric field effect has been found largely below expectations. Superconducting to insulating transitions were observed only in samples with a doping exactly at the separation between the two electronic phases [11, 12]. Only recently shifts of T_c up to 10 K were found in $YBa_2Cu_3O_7$ [8] and $NdBa_2Cu_3O_7$ (NdBCO) [9] thin films.

In this paper we present experimental results on the field effect doping of NdBCO thin films characterized by a carrier density near the superconducting–insulating transition. By realizing prototypal field effect devices (FED) characterized by a controlled number of CuO_2 layers, we were able to fine tune the characteristics of HTS films and to follow the SIT in unprecedented detail, hardly achievable using the chemical doping method. The results confirm that field effect doping modifies the transport properties of HTS thin films in a way which resembles strongly the effect of chemical doping, but without changing the chemical disorder or the structure. The analysis of the data supports the idea that, near the critical doping, HTS thin films are phase-separated into superconducting and weakly insulating regions. Moreover, the electric field doping modifies the distribution between these competing phases and the SIT appears as a continuous phase transition as a function of the doping.

2. Device characterization

NdBCO films were deposited by high oxygen pressure diode sputtering on 10×10 mm^2 $SrTiO_3(100)$ single crystals. The substrates were etched in a BHF solution (pH $=$ 5.5) and, just before the deposition, annealed at 950 °C in 10 Torr of pure oxygen in order to clean and to reconstruct the terrace structure. Friction and topography measurements, performed in contact mode, show well-ordered TiO_2-terminated and slightly vicinal surfaces with typical terrace widths of 200 nm. The best NdBCO films were deposited at a total pressure of 1.7 Torr, composed of 95% of oxygen and 5% of argon. The optimum deposition temperature was 920 °C and the growth rate was about 0.01 nm s^{-1}. The annealing procedure, which gives high critical temperature thin films, is different from that typically used in the case of YBCO films. The best samples are obtained by reducing, after deposition, the substrate temperature toward 500 °C with the O_2/Ar mixture flux and total pressure maintained constant at the values used during the deposition. At 500 °C the chamber is isolated and quickly filled by 400 Torr of pure oxygen. Finally the sample is oxygenated at these conditions for 1 h. To avoid oxygen losses, an amorphous insulating NdBCO layer is grown at room temperature on top of the structure. The unprotected surface of NdBCO films exhibit a structural relaxation after several days of exposure to the atmosphere (consistent with oxygen loss from the chains). Consequently the capping layer, which is completely amorphous, represents the protection necessary for the many measurements that should be done. With the NdBCO amorphous layer the sample is stable for months. However, the characteristics of protected and unprotected as-grown samples are very similar.

The rocking curves around the (0 0 1) and (0 0 5) reflections of all the films deposited are characterized by a full width at half-maximum of 0.030° and 0.080°, respectively, comparable with the resolution of our diffractometer. This result indicates a small orientation misalignment between individual islands in each sample. The structural coherence along the c axis of the NdBCO films extends to the entire thickness, as demonstrated by the presence of well-defined Pendellösung fringes around the (001) peak, even for films thicker than 100 nm (figure 1). From the period of the fringes it is possible to obtain a precise estimation about the film thickness even for a sample only 2 unit cells (uc) thin.

The structure of the NdBCO samples is pseudotetragonal [13], with the in-plane lattice perfectly matched with the STO substrate. As a consequence they are under strain (compressive along the b axis, tensile along the a axis). However, the in-plane mismatch is quite small (less than 1% in both in-plane directions), much smaller than the mismatch of YBCO deposited on STO substrates. As a consequence, no relevant effect of elastic stress is expected for these compounds. Notwithstanding, the transport properties are strongly dependent on the total number of unit cells, on the growth rate and on the exact interface structure [13]. As shown in figure 2, for films deposited at a deposition rate of only half a unit cell per minute, a superconducting to insulating transition occurs around 3 uc. A full superconducting sample, with T_c above 20 K, is obtained

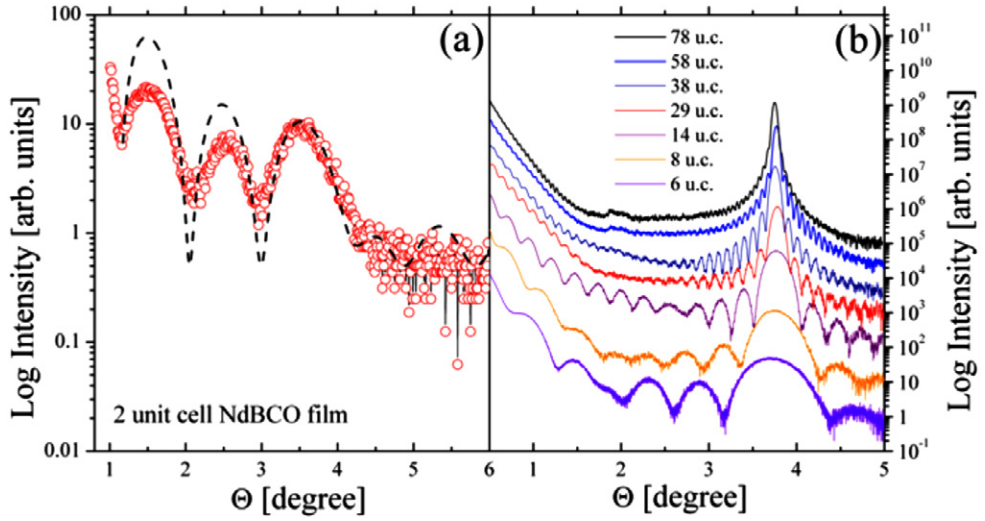

Figure 1. Low angle x-ray reflectivity oscillation on NdBCO thin films. (a) 2 unit cell film (red open circles). Superimposed as a dashed black line is a simulation corresponding to a 2 unit cells film. (b) NdBCO samples with thickness between 6 and 78 unit cells.

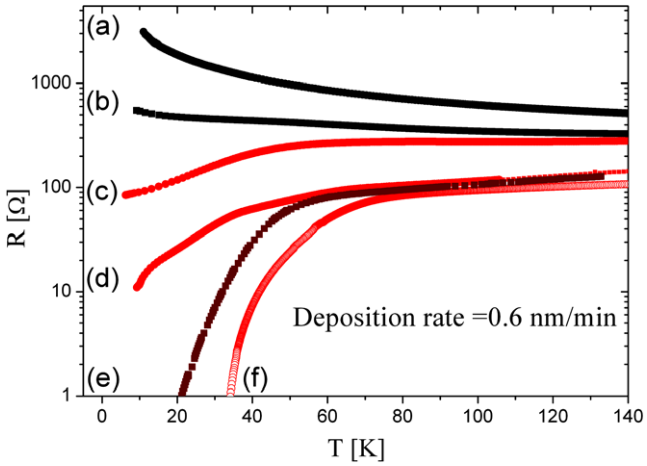

Figure 2. Temperature dependence of the channel resistance in NdBCO field effect devices composed of different numbers of unit cells: (a) 2 uc, (b) 2.5 uc, (c) 3.0 uc, (d) 3.5 uc on mixed terminated STO, (e) 3.5 uc and (f) 4 uc. Samples (a)–(f) are deposited on TiO_2-terminated STO substrate.

if at least 4 uc of NdBCO are deposited on top of a BHF-etched and TiO_2-terminated STO substrate, while for a similar thickness a sample deposited on a mixed terminated STO (not etched) is not superconducting.

In order to optimize each interface, the field effect devices (FED) have been fully realized *in situ* by sequential deposition of a thin NdBCO (001) film, of current-and voltage-evaporated gold pads realized by a shadow mask technique (the distance between the current and voltage pads are, respectively, 200 and 25 μm), and the gate electrode on the back of the 0.5 or 0.25 mm thick STO substrate. The quantum paraelectric STO single crystal is strongly insulating at low temperatures and is characterized by a very high dielectric constant, reaching $\varepsilon_r = 20\,000$ at low field and 4.2 K.

The devices are characterized by transport and charge measurements, using the experimental set-up sketched in figure 3(a). A source–drain current is injected in the NdBCO channel through a Keithley 6220 current source, while the source–drain resistance is measured through a Keithley 2182A nanovoltmeter. For each measurement the current direction is switched from positive to negative and the resulting voltages are averaged to get the value of the resistance. In the case of more than 5% difference between the two values of V_{DS} polarity, the data are considered affected by unknown systematic errors and discarded. Even very insulating samples show ohmic I_{DS} versus V_{DS} characteristics in the normal state. All the devices were studied in the linear regime where the condition $V_{gate} \gg V_{DS}$ holds.

The charge across the gate dielectric is measured through a Keithley 6517A electrometer, also equipped with a high voltage dc source. The leakage current in the device at cryogenic temperatures is always below 1–2 nA (not limited by the dielectric characteristics, but by the cabling assembly), allowing static charge to be measured with very high accuracy. In this way we could acquire simultaneously the channel resistance and the induced polarization, i.e. the charge induced at the interface. The latter can be directly transformed in holes per cm^2 or holes per CuO_2 planes, assuming that charges are transformed in carriers. As shown in figure 3(b), positive gate voltages (corresponding to hole depletion) decrease the conductivity of the device, while negative gate voltages (corresponding to accumulation of holes) increase it, in agreement with the idea that, by applying an electric field at the interface, it is possible to control the carrier density of the HTS hole-doped thin films. Similarly in figure 3(c) we report a typical R_{DS} versus gate voltage characterization of the device, used to quantitatively correlate the changes in the resistance with the amount of charge induced at the interface. As is apparent from the figure, hole depletion in a strongly insulating 1.0 uc sample is very effective in decreasing the sample conductivity, while the effect of hole accumulation is less pronounced, resulting in an asymmetric gate voltage dependence of the channel resistance. Note that we should

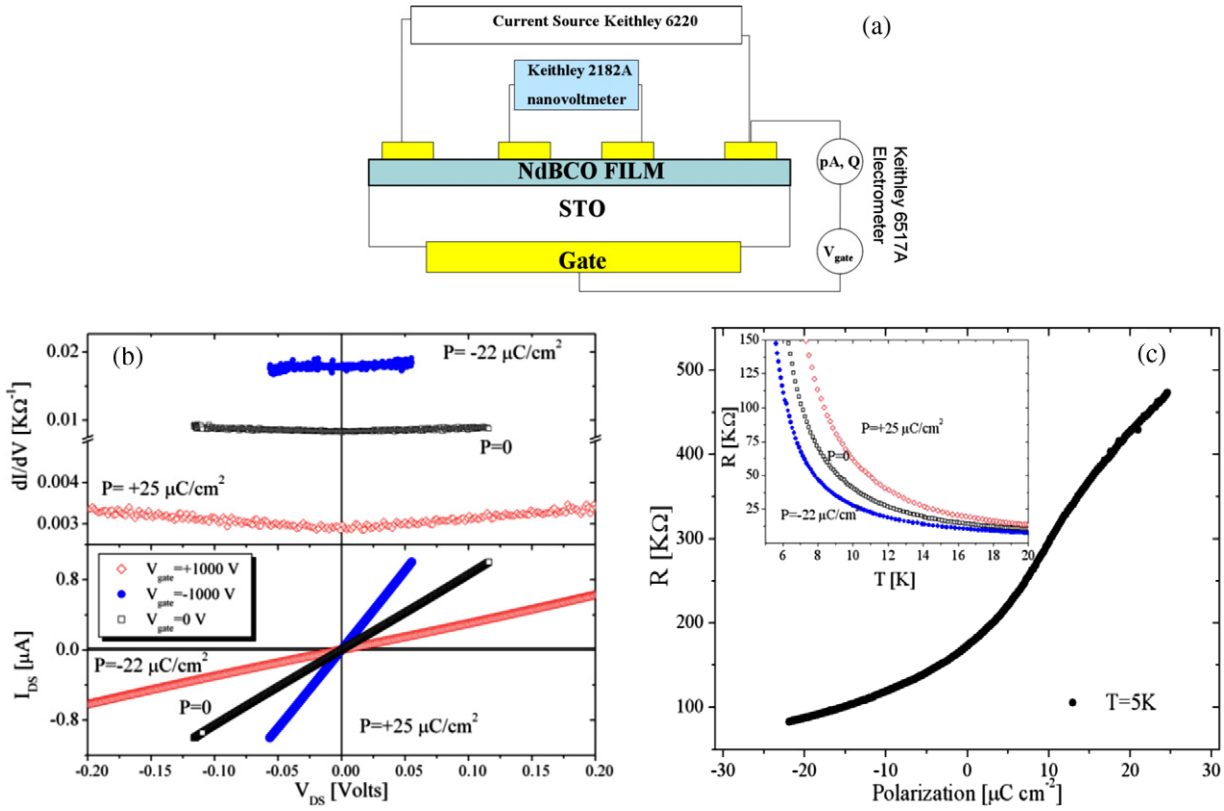

Figure 3. (a) Experimental set-up used to characterize the transport properties of the devices. (b) Conductance and I_{DS} versus V_{DS} characteristics of a 1 uc NdBCO insulating film for different measured polarization. (c) Channel resistance R versus the measured polarization of the 1 uc NdBCO FED measured at 5 K. In the inset the temperature dependence of the channel resistance for positive and negative polarization is shown.

expect a change of the carrier doping to switch the sample to the superconducting state. Indeed, even assuming that these carriers are distributed uniformly in the CuO_2 planes composing this thin film, $\pm 20\ \mu C\,cm^{-2}$ corresponds to a change in the number of carriers per CuO_2 planes of $\Delta p_{pl} = \Delta n_s \times (\text{Area } CuO_2 \text{ plane})/2 = \pm 0.05$ holes/CuO_2 plane.

The result suggests that the doping mechanism is much more complicated then expected. Indeed, recently we showed that the microscopic mechanism leading to the field effect doping of NdBCO is very similar to chemical doping: the charges induced are mainly created in the CuO chains (in the charge reservoir) and then partially transferred to the CuO_2 planes [14]. This is analogous to the general mechanism governing the charge transfer in the whole HTS family. As a consequence, the doping of the CuO_2 planes is rather indirect and occurs through partial charge transfer from the chains to the planes of a fraction of the total induced charge. This result implies that the number of carriers induced by the electric field is much lower than expected, explaining many previous observations, including the limited shift of T_c observed in optimal samples, and the difficulty in obtaining a complete switching between superconducting and insulating phases (and vice versa).

3. Experimental results: field effect doping

In figure 4 the experimental results obtained on FED characterized by a variable number of NdBCO layers composing the drain to source channel are summarized. From the data we can notice that it is possible to follow the region of the phase diagram across the SIT with unprecedented detail. However, in none of the samples studied using the STO substrate as gate dielectric, were we able to get a complete superconducting to insulating transition. This is at odds with the estimation of the expected doping based on the measured charges accumulated at the interface. In the hypothesis of complete transfer of the charges to the CuO_2 plane, a switching between superconducting and insulating phases is expected in each of the samples studied. Indeed the carriers are not transferred directly to the CuO_2 planes, but only a fraction of them fill the Zhang–Rice band. In the following paragraph we will analyze the experimental results in greater detail, starting from the study of the T_c modulation in the superconducting state and of the field effect doping of strong insulating devices. Finally we will consider the case of NdBCO films located near the critical doping separating the superconducting and the insulating regions of the HTS phase diagram.

3.1. Superconducting critical temperature modulation

Modulation of the critical temperature in NdBCO thin films is demonstrated in figure 5(a), where the temperature and gate voltage dependence of the resistivity and of the induced charge of a 3.5 uc FED deposited on 0.25 mm thick STO substrate are shown. The device is characterized by a zero resistivity

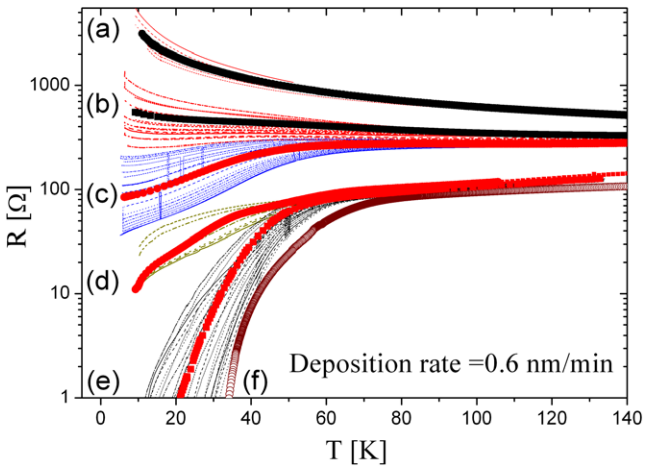

Figure 4. Summary of the field effect results on different NdBCO FEDs composed of different numbers of unit cells. Scatter data are obtained at zero gate voltage, while the thin dashed lines correspond to the data obtained by field effect doping. The labels (a)–(f) are the same as used in figure 2.

$T_c \cong 20$ K without a gate field applied. It is possible to notice that the charge induced is not constant as a function of the temperature and it is a nonlinear function of the gate voltage (figure 5(b)). Consequently, to correctly interpret the data, it is fundamental to know how the device is behaving by evaluating the induced charges. Providentially, the strongly nonlinear characteristic of the STO dielectric is smoothed out at relatively small electric field (gate voltages >50 V). As a consequence, the shape of the temperature dependence of the resistance is not affected drastically in the temperature range typical of the transition. In particular, at low temperatures and for a given gate voltage, the charge is effectively constant, and consequently the doping is also supposed to be constant. We have estimated a modulation of the critical temperature ΔT_c between 20 K (1 μV criteria) and 15 K (0.1 μV criteria), which represent remarkable values among the field effect results reported until now on HTS superconductors. Consequently we can effectively conclude that we are doping the CuO_2 planes in a very similar way to chemical doping.

To estimate the expected doping, and consequently the expected T_c shift, it is necessary to know how the induced charges distribute among the various CuO_2 planes, which are between 6 and 8 in this sample. It is common to estimate the electric field penetration using the Thomas–Fermi model, which assumes that the carriers in the CuO_2 planes screen the electric field. As a consequence, taking into account a reasonable estimate for the carrier density in our device, we have a penetration depth below 1 nm, i.e. less than one unit cell. Therefore, we expect that the carriers are transferred to the first two CuO_2 layers at the interface with STO. On the basis of this assumption, the number of holes per CuO_2 planes at the interface with STO should change from a value around 0.06 to a value higher than 0.10, i.e. a large region of the HTS phase diagram should be accessible in the accumulation mode. In the case of charge depletion, the shunting effect of the layers not facing the interface, that are believed to have higher doping [15], would clearly reduce the field effect for positive gate voltage, which is not observed. Therefore the data indicate that the carriers are distributed among more than one unit cell. Supposing that the first two unit cells are doped uniformly, we are still unable to explain the data quantitatively. Indeed, on the basis of the general phase diagram, a shift of T_c equal to 15 K corresponds to the injection of 0.03–0.04 holes per CuO_2 planes, i.e. to about 1/3 of the total induced charges. This value is in good agreement with the ratio between the fraction of charges transferred to the Cu(1)O chains and to the CuO_2 planes estimated by x-ray absorption spectroscopy [14]. However, it is important to underline that, without an independent assessment regarding the electric field penetration depth, a quantitative comparison between the electric field doping and chemical doping remains elusive. This is an important issue to consider in the interpretation of the field effect experiments when samples thicker than one unit cell are used in a back-gate configuration. A possibility to circumvent this problem consists in realizing a sandwich

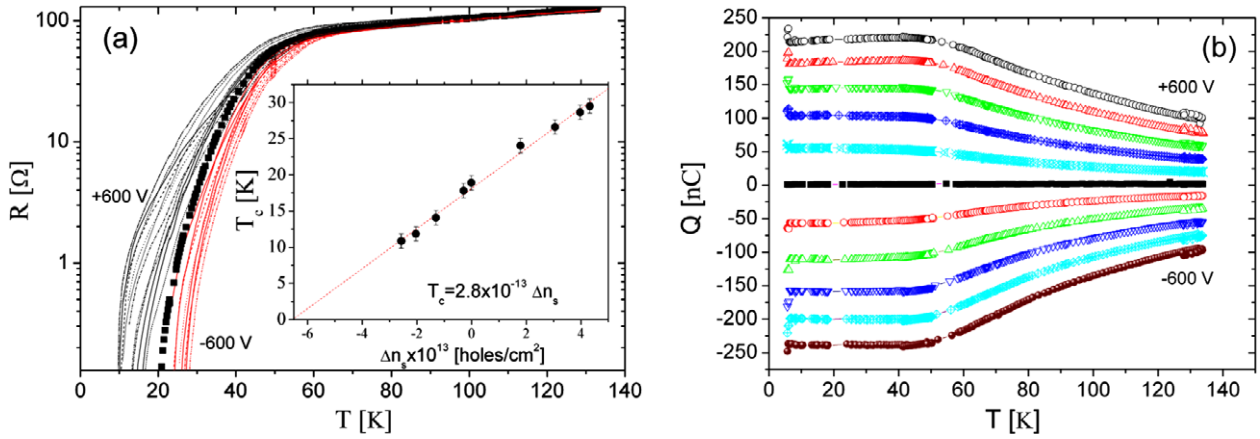

Figure 5. (a) Analysis of the field effect doping on 3.5 uc superconducting sample. Black filled symbols are obtained at zero gate voltage, while black lines, on the left of the filled symbols, correspond to positive (hole depletion mode) and grey lines (red), on the right of the filled symbols, are for negative gate voltages (hole accumulation mode). In the inset the T_c dependence on the measured surface charge overlapped with a linear fit. (b) Temperature dependence of the charge induced in the device measured during the transport data acquisition of (a).

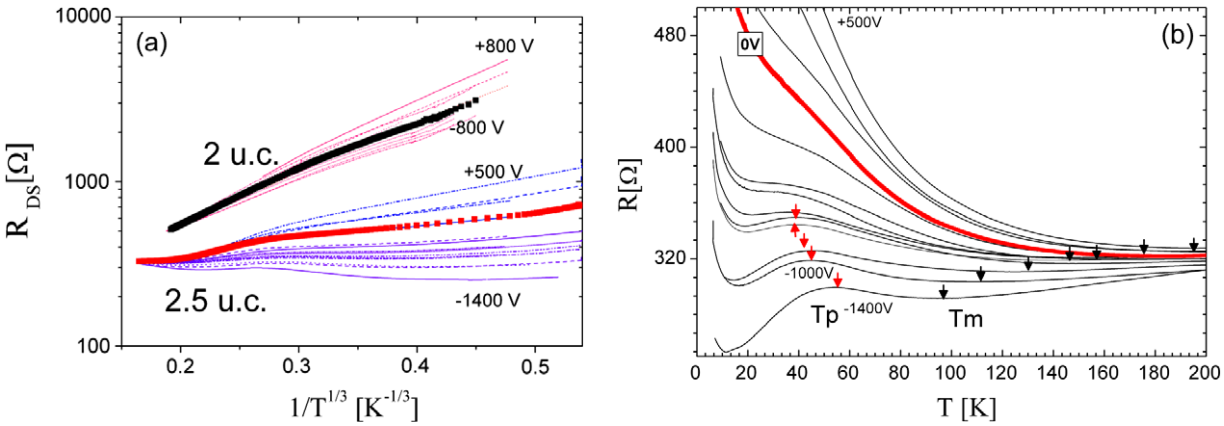

Figure 6. (a) Analysis of the field effect doping on insulating 2.0 uc and 2.5 uc samples. The data are plotted as Log(R) versus $(1/T)^{1/3}$ to highlight the VRH Mott 2D characteristics. The 2.5 uc sample undergoes a metal/superconducting–insulating transition by field effect doping. Black and red squares are data from a zero gate voltage on the 2.0 uc and 2.5 uc samples, respectively. Dashed lines represent the evolution as a function of the gate voltage. (b) Temperature dependence of the resistance in the 2.5 uc device, showing the insulating to (incomplete) superconducting transition. The red thick line corresponds to the zero gate voltage data, while black thin lines are the data at various gate voltages. The arrows indicate the position of the peaks (T_p, red) and of the minimum (T_m, black).

symmetric structure, where a dielectric is also deposited on the top of the thin film constituting the channel.

Before concluding this part, we should emphasize that we observe a linear dependence of the critical temperature as a function of the induced charges, as shown in the inset of figure 5(a), in both hole accumulation and hole depletion regimes. It is generally believed that, on the underdoped side of the phase diagram, the T_c of cuprates should follow the Uemura relation, where it is effectively proportional to $1/\lambda^2$ and consequently to the carrier density and to Δn_s. In [9] Matthey *et al* reported on the field effect experiment on NdBCO thin films and showed that the Kosterlitz–Thouless temperature estimated by the experimental data was linear as a function of the induced charge. Our data are not sufficiently accurate to effectively verify this finding: in particular, we cannot estimate reliably the Kosterlitz–Thouless transition temperature. However, our data support this picture in a range of doping that is larger than the one reported in [9] and for both hole accumulation and hole depletion modes. On the other hand, this finding is not necessarily a proof that the SIT in this system is a 2D quantum phase transition belonging to the 3D XY universality classes [16]. It can be an indication of this, but it is not a sufficient condition (see below).

3.2. Modulation of the resistivity in the insulating phase and superconducting–insulating transition

The temperature dependence of the resistivity in insulating thin NdBCO films is well explained by a variable range hopping (VRH) mechanism of conduction in the 2D Mott limit. This is demonstrated in figure 6(a), where $\log(\rho)$ shows a linear dependence as a function of $(1/T)^{1/3}$ down to 5 K. The electric field doping modifies the slope of the experimental curves, which is related to a temperature T_0 defining the degree of carrier localization in the compound [17]. Note that a similar formula is applicable also to the case of carriers in the form of small polarons. From the data we notice that the slope of the VRH curves decreases when the gate voltage is swept between positive and negative values. The change in the slope is correlated to an increase of the localization length of the carriers, as already reported in [18]. Notably, approaching the SIT from the insulating side, we observe a deviation from the experimental VRH law. This is particularly shown in the temperature dependence of the resistivity of the 2.5 uc FED, which is located at the boundary between the insulating and the superconducting phase. This sample is characterized by a non-monotonic temperature dependence of the resistivity at zero gate voltage. In particular, the positive slope, related to the insulating character of the thin NdBCO channel, increases below 40 K (figure 6(b)). However, the gate voltage dependence reveals very interesting changes in the resistivity. In particular, by applying sufficiently large positive gate voltages, corresponding to hole depletion, the non-monotonic behavior disappears. At $V_{gate} = +500$ V, a power law of the form $\rho = aT^q$ or a $\rho = \log(1/T)$ function (sometimes ascribed to quantum localization) are able to reasonable fit the data. In this region the VRH mechanism of conduction is replaced by a weakly insulating characteristic. On the other hand, for opposite gate voltages, the non-monotonic characteristic becomes more pronounced, and the change of curvature is replaced by a local maximum at T_p in the temperature dependence of the resistivity followed by a transition to an incipient superconducting state. Simultaneously, we can see that at higher temperatures a local minimum, T_m, develops in the experimental curves. It is interesting to note that, while T_p shifts to higher temperatures as a function of the doping, T_m moves in the opposite direction. These data reveal a very interesting feature of thin NdBCO samples near the SIT. Competing phases, in particular a weakly insulating and a superconducting phase, coexist simultaneously. Another indication of the presence of mesoscopic phase separation comes from the fact that for some electric fields we observe a clear re-entrant insulating behavior at low temperatures. The ratio between the superconducting

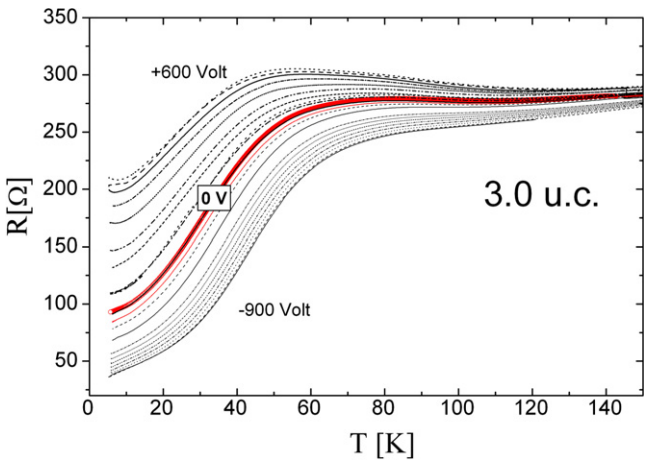

Figure 7. Temperature dependence of the resistance in the 3.0 uc device as a function of the electric field. Note the appearance of a peak and of a minimum in the resistivity for gate voltages higher than −100 V.

and insulating phases is modified by the electric field, and the data suggest that it is possible to switch from one phase to the other in a continuous fashion. The results are confirmed by analyzing 3.0 uc FED, being not fully superconducting at 4.2 K. The 3.0 uc samples shows analogous signatures of competing phases (figure 7). While applying the electric field we were unable to switch the sample to the insulating state; all the other features of a phase-separated system are clearly shown. In particular, above a gate voltage of −100 V, the resistivity shows a maximum T_p and a minimum T_m, analogous to those observed in a 2.5 uc sample. By inducing a sufficient number of holes, the local maximum and minimum disappear and merge at the onset of the superconducting transition. Here the signatures of competing phases disappear, and the sample is composed only of superconducting regions. In contrast, by taking out holes from the sample, T_p and T_m shift to lower and higher temperatures, respectively. This result is in agreement with the fact the critical temperature of the superconducting regions decreases, lowering the carrier doping. In [19] a similar phenomena was found in $Bi_2Sr_{2-x}La_xCaCu_2O_8$ samples, with doping modified by oxygen stoichiometry. There a direct proportionality between T_p and T_c was found.

The similarity between the 'field effect doping' and chemical doping phase diagrams near the SIT transition is remarkable. The characteristic temperature and chemical doping dependence of the resistivity has been observed in other HTS superconductors, i.e. in $Bi_2Sr_{2-x}La_xCaCu_2O_8$, $YBa_2Cu_3O_7$ and $La_{2-x}Sr_xCu_2O_4$ crystals and films [19–22]. This is a further proof that field effect doping and chemical doping have a common microscopic mechanism.

4. Discussion

The superconducting–insulating transition in two-dimensional superconductors is considered an example of continuous quantum phase transitions [16]. A reduced dimensionality is achieved in metals by depositing ultrathin films. HTS are considered quasi-two-dimensional superconductors, with transport confined to the CuO_2 planes. Therefore our ultrathin NdBCO films can be considered strongly 2D systems and consequently the SIT induced by doping in these materials could belong to the category of continuous quantum phase transitions. We have noticed that T_c of our superconducting samples is mostly linear as a function of the surface charge induced by the electric field. However, we have also demonstrated that the charge induced does not correspond directly to the holes injected into the CuO_2 planes. However, there are indications that the proportionality between the total charge and the number of holes injected are still valid in the case of '123' compounds [14]. Consequently, this result could indicate that the superconducting transition in these materials belongs to the 3D XY universality class. However, overall consistency should be checked by an analysis of the 2D quantum scaling near the SIT. A finite-size scaling of the experimental observable as a function of the field effect would be strong evidence of this mechanism. The scaling theory states that the resistance R of 2D samples, above and below a critical value K_c of a tuning parameter K, should obey the functional form

$$\frac{R}{R_c} = F\left[\left|\frac{K - K_c}{T^{\nu z}}\right|\right]. \quad (1)$$

Here F is the scaling function, R_c is the value of the resistance at the critical point, ν is the correlation length critical exponent and z is the dynamical critical exponent. While in amorphous BCS superconductors successful finite-size-scaling analysis, consistent with 2D quantum transition, was reported [6], this was not the case for the HTS. We have tried to apply the finite-size-scaling analysis to our data. In our case, the tuning parameter is the gate voltage or the induced surface carriers. As a first step, we determine the critical parameters from isotherms of the resistance versus the gate voltage in a 2.5 uc sample. The data show crossing at values of the gate voltage V_c of about −1000 V and critical resistance $R_c = 318\ \Omega$. As a second step we have assumed that the 3.0 uc sample at $V_g = +600$ V and the 2.5 uc NdBCO at $V_g = -1400$ V have similar doping. This hypothesis is reasonable since T_p and the high temperature resistances of the two devices are similar.

As a consequence of this analysis, we can notice that the data do not scale with any values of the critical exponents' product νz. As shown in figure 8, the best collapse is obtained with rather high νz values of 1.8, which on the other hand would indicate 2D quantum percolation and not a quantum phase transition belonging to the universality classes of 3D XY models and boson-Hubbard models in the absence of disorder [16]. Moreover, strong deviation between various experimental curves is noticed in the transition region. Similar results are obtained by using the induced charge (measured simultaneously to the resistance), instead of the gate voltage, as the tuning parameter. It is therefore evident that finite scaling in the electric-field-induced SIT transition in underdoped NdBCO films is not satisfying. It is likely that, since in the HTS the onset of the phase transition occurs at relatively high temperatures, quantum effects, which of course have an

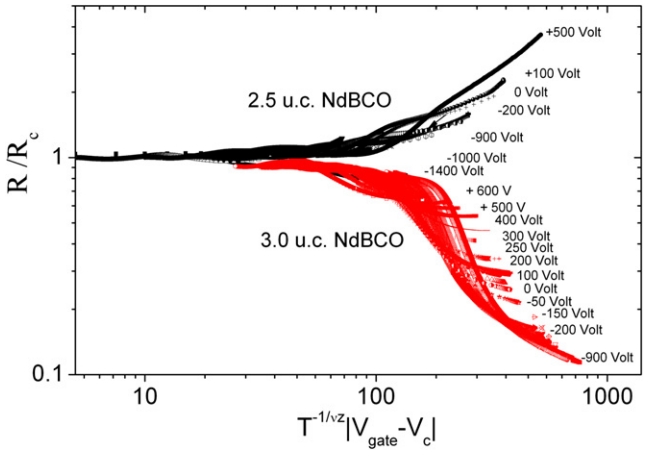

Figure 8. Attempt to apply the 2D scaling theory on the field effect doping data acquired on 2.5 uc and 3.0 uc NdBCO thin films. The scaling is not satisfying even for the rather high values of νz values of 1.8 used in the plot.

important role in the physical phenomena, could be washed out by thermodynamic (classical) fluctuations.

From this analysis it emerges that a 2D quantum phase transition is not able to explain the superconducting to insulating transition in our NdBCO thin films. On the other hand, the data suggest that critical samples are characterized by the coexistence of two competing phases on a mesoscopic scale, i.e. a weakly insulating phase and a superconducting phase. Doping modifies the ratio between the two phases. Consequently, around the phase transition, the HTS appear to be phase-separated. It is very interesting to notice that, while the electric field is uniform on a mesoscopic scale, the carriers distributed within the CuO_2 planes are not. This means that the added charges intrinsically distribute in hole-rich and hole-poor regions, independent of the mechanism being by electric field doping or chemical doping. This suggests that the phase separation is intrinsic to the HTS near the critical doping. However, there are different questions that remain to be answered concerning the microscopic characteristic of the two competing phases. The fact that in the insulating region of the phase diagram there is a crossover from a weakly insulating phase to a Mott insulating one is also quite suggestive. One possible proposal is that the insulating phase is composed by Cooper pairs localized because of the strong charging energy of the individual 'islands', as proposed recently in amorphous superconductors [23]. In this state the charge, or the total number of Cooper pairs, is a well-defined number. This state is dual to the superconducting phase, where the charge is not defined, while the phase of the order parameter is. Further studies in this direction are needed to verify this possibility: however, to avoid the complication associated with the strong thermal (classical) fluctuations experiments at very low temperatures are required.

Acknowledgments

M Salluzzo, G M De Luca, A Gambardella and R Vaglio acknowledge the support from the EU under project Nanoxide, contract no. 033191.

References

[1] Chakravarty S, Halperin B I and Nelson D R 1988 *Phys. Rev. Lett.* **60** 1057
[2] Lee P A, Nagaosa N and Wen X-G 2006 *Rev. Mod. Phys.* **78** 17
[3] McElroy K, Lee J, Slezak J A, Lee D-H, Eisaki H, Uchida S and Davis J C 2005 *Science* **309** 1048
[4] Hossain M A *et al* 2008 *Nat. Phys.* **4** 527
[5] Ohtomo A and Hwang H Y 2004 *Nature* **427** 423
[6] Kevin Parendo A, Sarwa K H, Tan B, Bhattacharya A, Eblen-Zayas M, Staley N E and Goldman A M 2005 *Phys. Rev. Lett.* **94** 197004
[7] Rufenacht A, Locquet J-P, Fompeyrine J, Caimi D and Martinoli P 2006 *Phys. Rev. Lett.* **96** 227002
[8] Logvenova G Yu, Schneider C W, Mannhart J and Barash Yu S 2005 *Appl. Phys. Lett.* **86** 202505
[9] Matthey D, Reyren N, Triscone J-M and Schneider T 2007 *Phys. Rev. Lett.* **98** 057002
[10] Mannhart J, Schlom D G, Bednorz J G and Muller K A 1991 *Phys. Rev. Lett.* **67** 2099
[11] Ahn C H, Gariglio S, Paruch P, Tybell T, Antognazza L and Triscone J-M 1999 *Science* **284** 1152
[12] Cassinese A, De Luca G M, Prigiobbo A, Salluzzo M and Vaglio R 2004 *Appl. Phys. Lett.* **84** 3933
[13] Salluzzo M, De Luca G M, Marré D, Putti M, Tropeano M, Scotti di Uccio U and Vaglio R 2005 *Phys. Rev.* B **72** 134521
[14] Salluzzo M, Ghiringhelli G, Cezar J C, Brookes N B, De Luca G M, Fracassi F and Vaglio R 2008 *Phys. Rev. Lett.* **100** 056810
[15] Logvenov G Yu, Sawa A, Schneider C W and Mannhart J 2003 *Appl. Phys. Lett.* **83** 3528
[16] Sondhi S L, Girvin S M, Carini J P and Shahar D 1997 *Rev. Mod. Phys.* **69** 315
[17] Perez-Garrido A, Ortuno M, Cuevas E, Ruiz J and Pollak M 1997 *Phys. Rev.* B **55** R8630 and references therein
[18] Salluzzo M, Cassinese A, De Luca G M, Gambardella A, Prigiobbo A and Vaglio R 2004 *Phys. Rev.* B **70** 214528
[19] Seongshik Oh, Crane T A, Van Harlingen D J and Eckstein J N 2006 *Phys. Rev. Lett.* **96** 107003
[20] Semba K and Matsuda A 2001 *Phys. Rev. Lett.* **86** 496
[21] Ando Y, Boebinger G S, Passner A, Kimura T and Kishio K 1995 *Phys. Rev. Lett.* **75** 4662
[22] Ono S, Ando Y, Murayama T, Balakirev F F, Betts J B and Boebinger G S 2000 *Phys. Rev. Lett.* **85** 638
[23] Vinokur V M, Baturina T I, Fistul M V, Mironov A Yu, Baklanov M R and Strunk C 2008 *Nat. Lett.* **452** 613